PROTON MAGNETIC RESONANCE IN β-PHASE PALLADIUM HYDRIDE

Robin L. Armstrong

Department of Physics

University of Toronto

Toronto, Canada, M5S 1A7

Contents

I. Introduction 116

II. Spin Temperature Hypothesis 116

III. Hydrogen Atom Tunneling 117

IV. Proton Lineshape in the Intermediate Temperature Regime 118

V. Low Temperature Proton Lineshape 121

VI. Conclusion 124

VII. References 124

I. Introduction

Palladium hydride (PdH_X) is an alloy of significant intrinsic interest and of potential practical importance. On the one hand it is a simple alloy which exhibits marked quantum behaviour; on the other hand it is an example of a transition metal hydride which could be of interest for hydrogen storage. The experiments that will be discussed were carried out on three samples of palladium hydride prepared in the β-phase with different concentrations X of hydrogen but made from the same batch of palladium foil, 0.002 cm in thickness.

Proton magnetic resonance experiments carried out on this non-stoichiometric alloy provide information on the spatial distribution of the hydrogen atoms in the structure, on the proton dynamics, on the magnitude and nature of the magnetic fields at the proton sites and their correlations and on the nature of the proton-electron coupling. Several examples of the results of such studies carried out in my laboratory will be presented.

II. Spin Temperature Hypothesis [1]

It is not immediately obvious that the spin temperature hypothesis will be valid for the protons in this non-stoichiometric alloy. The question is whether the variation in the local field from site to site is sufficient to inhibit the energy conserving flip-flop transitions required to establish a uniform spin temperature throughout the sample. To test the hypothesis an experiment is performed in which an rf pulse is applied suddenly and the proton spin magnetization is detected following the pulse as a function of the offset frequency. For a short pulse the spin system can be considered to be isolated from the lattice and on the assumption of the existence of a spin temperature it follows that the x-component of the magnetization M_x is given by

$$\frac{M_x}{M_0} = \frac{hH_1}{h^2 + H_1^2 + H_L'^2} \qquad (1)$$

where h is the frequency offset, H_1 is the amplitude of the rf field during the pulse, H_0 is the amplitude of the external magnetic field and H_L' is the average local field in the rotating frame. For a long pulse thermal contact with the lattice can not be neglected and

$$\frac{M_x}{M_0} = \frac{hH_1}{h^2 + \lambda H_1^2 + \delta H_L'^2} \qquad (2)$$

where the parameters λ and δ are defined by

$$\lambda = T_{1z}/T_{1x} \text{ and } \delta = T_{1z}/T_{1D}.$$

Figure 1 shows the data measured at 40 K for the sample with X = 0.75 for a short rf pulse (crosses) and a long rf pulse (dots). By fitting equation (1) to the dots a value of $H_L'^2 = 45 \pm 2$ kHz^2 was obtained. This compares with the value 43 kHz^2 calculated on the assumption of a random distribution of protons on fcc sites coupled solely by a dipolar interaction. Using this value of H_L' and assuming that $\lambda = 1.0$, fitting equation (2) to the crosses yields a value of $\delta = 2.7 \pm 0.2$.

For dipolar interactions the parameter δ must lie in the range $2 \leq \delta \leq 3$. The lower limit corresponds to no correlation between the fluctuating magnetic fields at neighbouring sites; the upper limit to complete correlation. The result indicates that a significant amount of correlation exists. This conclusion was checked by an independent measurement of the parameter δ obtained from measurements of T_{1z} and T_{1D}.

The fact that the experimental data can be well represented by equations (1) and (2) with reasonable values of the parameters constitutes an experimental proof of the validity of the spin temperature hypothesis for the proton spin system in PdH_x.

III. Hydrogen Atom Tunneling[2,3]

No direct measurement of hydrogen tunneling had been reported. It was decided to attempt a magnetic resonance detection of the tunneling using a technique known as spin polarization torsional spectroscopy (SPOTS). The selection rule dictates that only tunneling which involves the simultaneous motion of small groups of hydrogen atoms can be detected. There was no way to know a priori whether or not such would be the case in a many body system such as β-phase PdH_x.

The pulse sequence consists of a $\pi/2$ pulse followed by a phase shifted spin locking pulse. This excitation sequence results in the creation of a non–equilibrium state in the rotating reference frame. The state oscillates and decays away in a time of the order of magnitude of 100 μsec thereby giving rise to a quasi–equilibrium state describable by spin temperature. The damped oscillation at frequency $\omega \approx 2\gamma H_1$ corresponds to the back and forth exchange of energy between Zeeman and spin-spin reservoirs. It is readily observable if the amplitude H_1 of the locking pulse is chosen to be larger than but comparable to the local field in the rotating frame H_L'. The decay is mapped out point by point as the length of the locking pulse is incremented in steps.

The presence of low frequency tunneling modifies the rigid lattice response. The SPOTS technique exploits this modification to yield experimental values of the tunneling splittings. In this case H_1 must be chosen to be much larger than H_L'. The Zeeman and spin–spin reservoirs are now not directly coupled but are indirectly coupled through a third reservoir associated with the tunneling levels. The effect of this intermediate coupling on the transient response is manifested through a modulation of the decay amplitude by sum and difference frequencies $\omega \pm \omega_T{}^i$ where $\omega_T{}^i$ is the ith tunneling frequency.

Figure 2(a) shows the non-equilibrium magnetization in the rotating frame, $< I_z >(t) = M_x/M_0$ for the sample with X = 0.80 as a function of the duration of the locking pulse incremented in steps $\Delta t = 1.5$ μsec. The solid line joins the data points; the dashed line is a rough guide to the eye indicating the modulation of the decay signal by the tunneling motion of the protons. Figure 2(b) shows the Fourier transform of these data. This spectrum displays a dominant doublet centred at about 80 kHz and with a splitting $\Delta f = 2 \times 16.5$ kHz. A second doublet of weaker intensity and with splitting $\Delta f = 2 \times 44$ kHz is also indicated.

Figure 3 shows the concentration dependence of the two lowest tunneling splittings deduced from three PdH_x samples. The fact that both tunneling frequencies decrease with increasing hydrogen concentration may simply be related to the reduction in

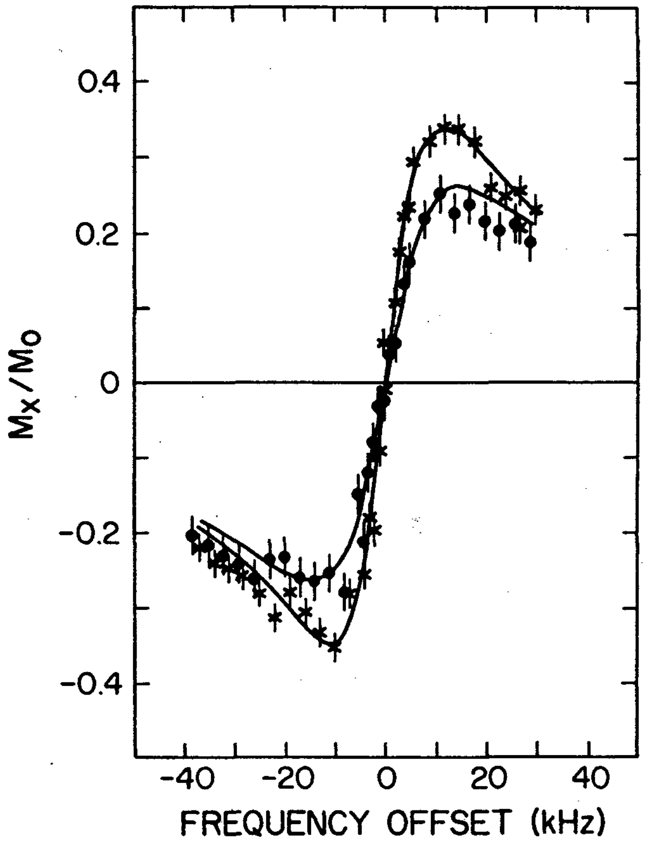

Figure 1: The proton spin magnetization ratio M_x/M_0 as a function of frequency offset for the PdH_x sample with X = 0.75 for spin temperature experiments using a 50 msec rf pulse (crosses) and a 3 sec rf pulse (dots) and with H_1 = 7.6 ±0.4 kHz. The solid lines are the theoretical fits to equations (1) and (2).

the number of vacant sites with increasing concentration. If so, the tunneling frequency should vary linearly with (1 - X); the straight lines indicate that this is approximately the case.

The tunneling frequencies are comparable to the proton dipolar coupling strength in frequency units and this fact must be reflected in the proton magnetic resonance line shape observed at this temperature.

IV. Proton Lineshape in the Intermediate Temperature Regime[4,5]

The proton free induction decay signal obtained at 40 K in a sample with X = 0.75 is shown by the dots in Figure 4.

The signal exhibits a beat pattern. An attempt was made to find an empirical mathematical representation of the data. The solid line is of the form

$$f(t) = f(0)\exp(-a^2t^2)J_{3/2}(bt)/(bt)^{3/2} \qquad (3)$$

where $J_{3/2}$ is a Bessel function of the first kind and a, b are constants. Expanding this function in powers of t and equating the resultant expression term by term with the moment expansion of the lineshape yields

$$f(t)/f(0) = 1 - (2a^2 + b^2/5)(t^2/2!) +$$

$$(12a^4 + 12a^2b^2/5 + 3b^4/35)(t4/4!)\cdots$$

$$= 1 - M_2(t^2/2!) + M_4(t^4/4!)\cdots \qquad (4)$$

In order to check the validity of this empirical form for short times (during the recovery time of the spectrometer) a magic echo experiment was carried out; the response should be identical to the free induction decay for short times. The data points indicated by crosses on Figure 4 were taken using this sequence. They fall on the empirical curve fitted to the free induction decay signal.

Therefore, the mathematical form of equation (3) may be used with confidence to determine the moments M_2 and M_4 using equation (4) and the moment ratio $\mu = M_4/M_2^2$. The results are given in Table 1. The theoretical values are calculated

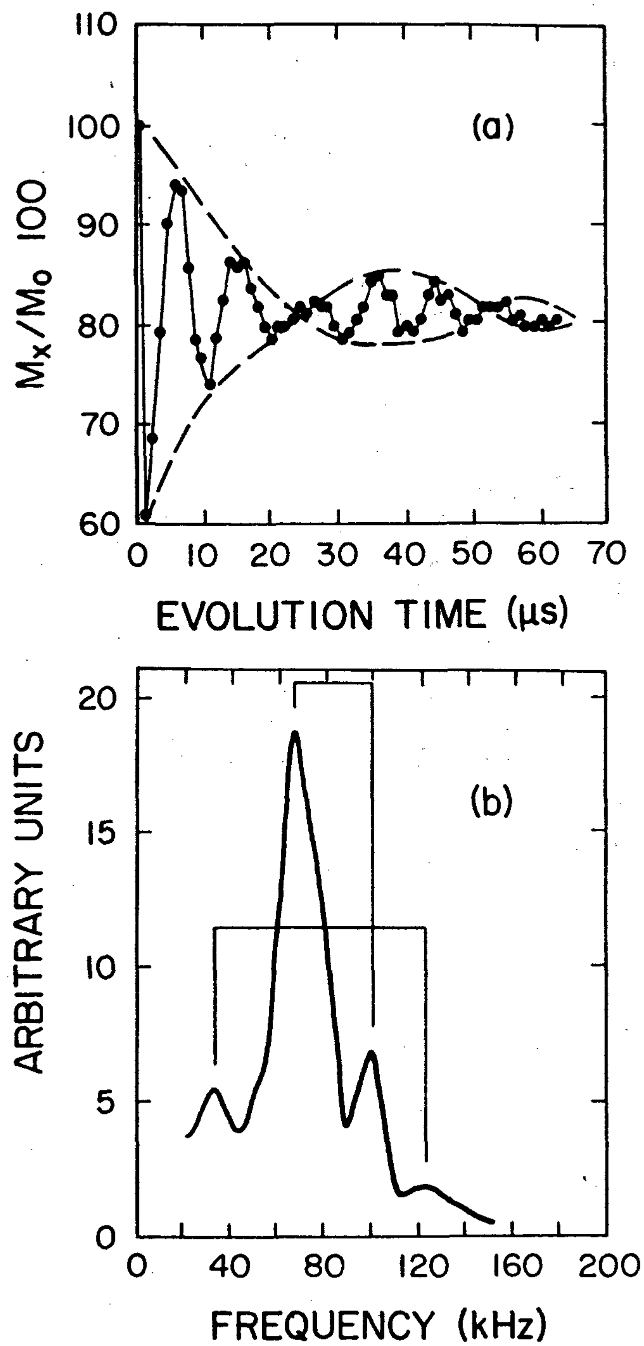

Figure 2: (a). Non-equilibrium proton spin magnetization ratio M_x/M_0 as a function of the duration of the locking pulse for the PdH_x sample with $X = 0.80$. The amplitude of the locking pulse was 8.40 ± 0.40 gauss. The dashed line is a guide to the eye to indicate the modulation. (b). Fourier transform of the transient data. Dominant and secondary doublets centered at about 80 kHz indicate tunneling splittings.

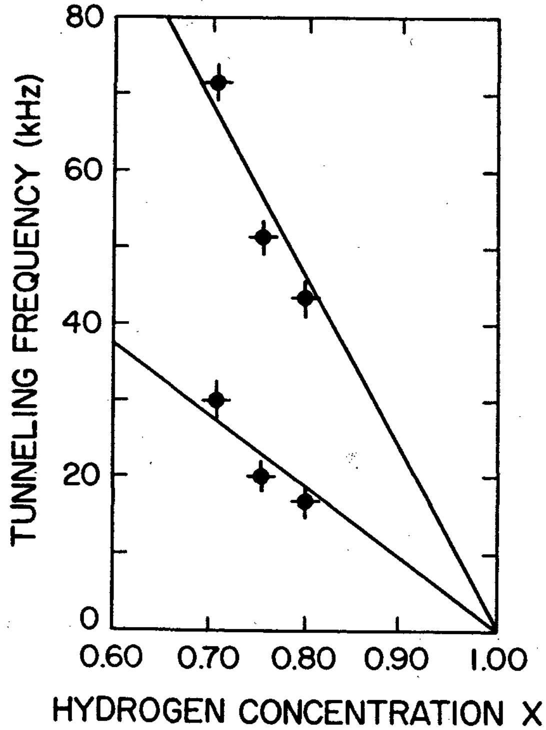

Figure 3: Concentration dependence of the two lowest tunneling frequencies in β-phase PdH_x. The straight lines are guides to the eye; they indicate a (1 - X) dependence.

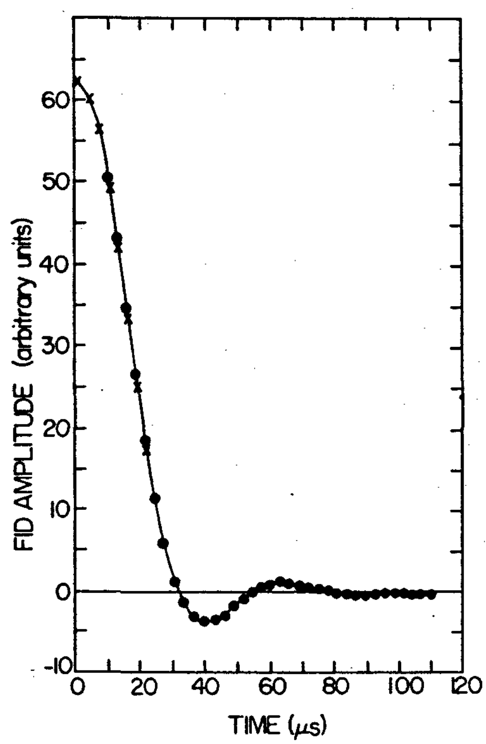

Figure 4: The proton free induction decay signal for the PdH_x sample with X = 0.75. The dots are experimental data and the full curve the fit to the empirical function given by equation (3). The crosses are data points obtained using a magic echo sequence.

on the assumption of random occupation of octahedral sites and dipolar interactions between occupied sites. The first thing to note is that the experimental and theoretical values of the moment ratio μ agree. This may be taken as confirmation of the neutron scattering result that the hydrogen atoms occupy the octahedral vacancies. That the measured moments themselves are smaller than the theoretical moments and increasingly so with decreasing concentration can be attributed to the hydrogen atom tunneling motion and its concentration dependence.

Examples of the lineshape recorded over the temperature range 30 to 80 K for the sample with $X = 0.71$ are given in Figure 5. The narrow central feature is believed to result from the tunneling of the hydrogen atoms in small groups. It has been shown that such correlated motion gives rise to transitions at the center of an absorption spectrum. Note that since this feature represents less than 5% of the total area of the lineshape and occurs at its center, therefore it contributes very little to the moments.

For a homogeneously broadened line such as results from an interaction bilinear in the spin operators, it is not possible to produce a Hahn echo. On the other hand, an interaction linear in the spin operators results in an inhomogeneously broadened line and a Hahn echo can be excited. A weak Hahn echo has been detected for the PdH_x samples. The obvious candidate for the scalar interaction responsible is the distribution of Knight shifts which occurs in a non-stoichiometric alloy. The Knight shift, as given by the zero crossing of Figure 1, is due to the local magnetic fields created at the proton sites by the conduction electrons. Figure 6 shows the frequency spectrum deduced from the Hahn echo observed in the sample with X = 0.71. The width at half height is 7.2 kHz which is approximately the width of the central feature in the spectra shown in Figure 5. The area under the echo is similar to that of the central feature. It is concluded that there is a strong relationship between the central feature in the proton magnetic resonance spectrum and the appearance of a Hahn echo, and that both features relate to the occurrence of low frequency hydrogen tunneling.

The inhomogeneity of the proton magnetic resonance spectrum at its center would be expected to result in a difference between the spin lattice relaxation time as measured at the center of the spectrum from that measured in the wings. Such is indeed the case.

V. Low Temperature Proton Lineshape[6]

Measurements of the proton free induction decay response in the temperature range between 10 and 30 K reveal a change in their shape with temperature. This is illustrated in Figure 7 for the sample with X = 0.75. At 10 K the free induction decay signal is gaussian, but as the temperature is increased the free induction decay signal gradually develops a beat structure. The signal at 25 K is the same as that observed throughout the range from 30 to 80 K. It should also be noted that the free induction decay is steeper at 10 K than at 25 K; the line is therefore wider at 10 K. To obtain the undistorted line shape at 10 K a magic echo sequence was used. The lineshape is a pure gaussian to within experimental error and has a second moment

$$M_2 = {\Delta_{1/2}}^2/4 = 160\text{kHz}^2 \qquad (5)$$

with $\Delta_{1/2}$ the width of the spectrum measured at half maximum. The result is independent of hydrogen concentration.

The rigid lattice theoretical second moment for a stoichiometric PdH sample neglecting any scalar interaction is 167 kHz^2; this is remarkably close to the experimental value. This result suggests that at 10 K the motion of the hydrogen atoms has been frozen out and that they tend to form stoichiometric clusters. The dimensions of such clusters need not be large.

A mechanism by which the free induction decay signal evolves from a rigid lattice gaussian shape at 10 K to a partially motionally averaged function that exhibits beats at 25 K is provided by thermal assisted tunneling. As an illustration we can consider a "two-well" model. The potential barrier describing the two wells and defined by the hydrogen-hydrogen interactions will not, in general, be symmetric as a result of the non-stoichiometry of the sample. That is, tunneling can not occur until the temperature is sufficiently high so that the thermal fluctuations broaden the energy levels of the two wells so that they match for some value of energy. The minimum thermal energy required to overcome

Table 1: Proton second and fourth moments and the moment ratio $\mu = M_4/M_2^2$

X	M_2		M_4		μ	
	Expt $(kHz)^2$	Theor $(kHz)^2$	Expt $10^3(kHz)^4$	Theor $10^3(kHz)^4$	Expt	Theor
0.80	123 ±3	134 ±2	35.8 ±1.4	40.4 ±1.1	2.4 ±0.1	2.3 ±0.1
0.75	108 ±1	125 ±2	27.0 ±1.0	35.7 ±1.1	2.3 ±0.1	2.3 ±0.1
0.71	91 ±2	119 ±2	19.1 ±2.0	32.1 ±1.1	2.3 ±0.1	2.3 ±0.1

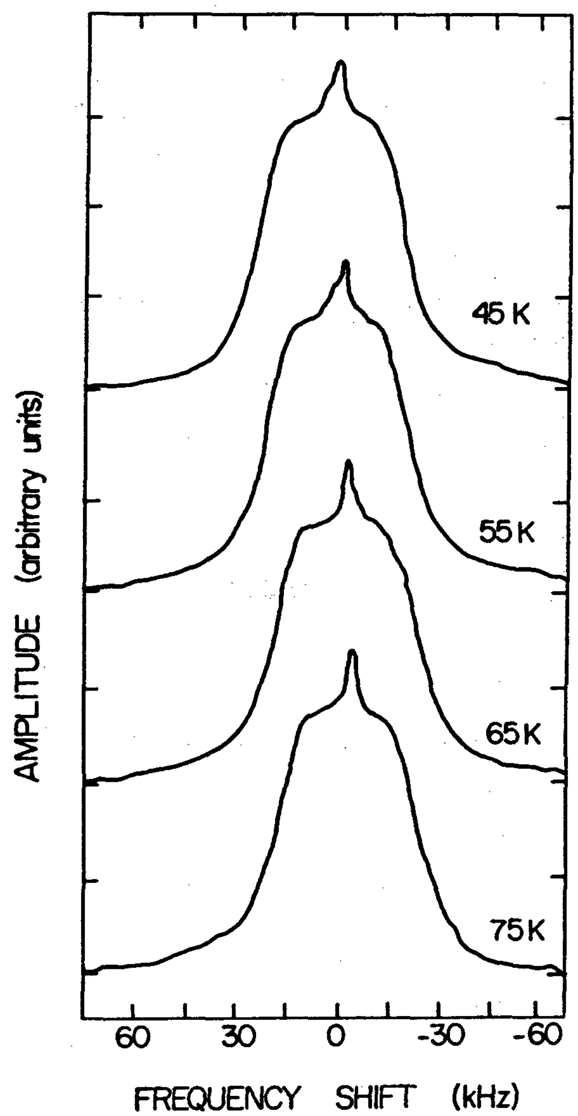

Figure 5: Examples of the proton spin absorption lineshape measured for the PdH_x sample with X = 0.71 in the temperature range 30 to 80 K. The width of the central feature at half height is about 7 kHz.

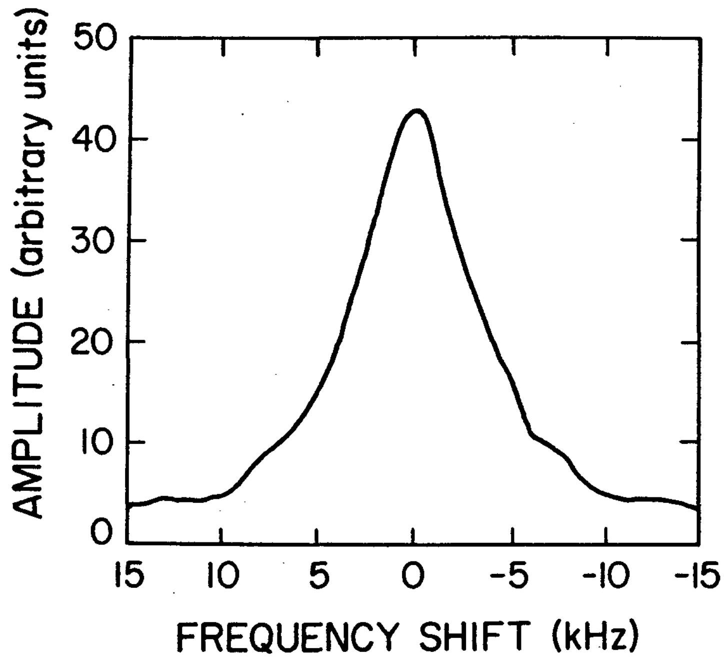

Figure 6: Proton spin absorption spectrum deduced from the Hahn echo for the PdH_x sample with X = 0.71 at 40 K. The spectral width at half height is 7.2 kHz.

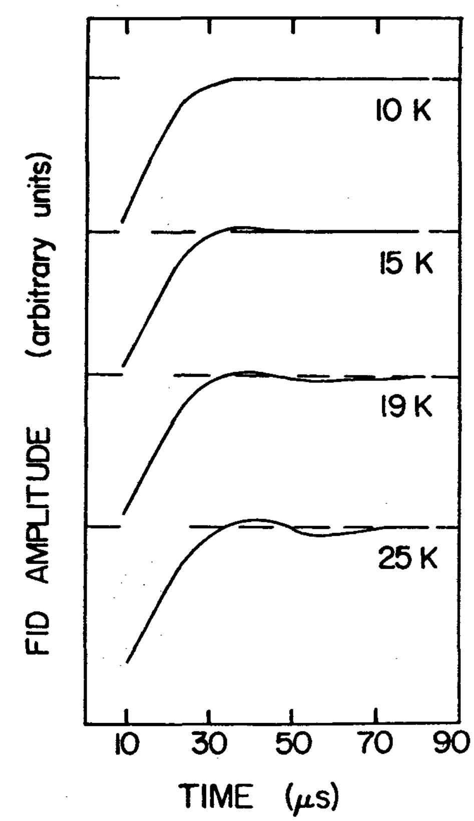

Figure 7: Examples of the proton free induction decay signal obtained from the PdH_x sample with X = 0.75 in the temperature range 10 to 30 K.

the asymmetry is roughly kT_0 with T_0 the average temperature at which the observed change takes place. For $T_0 = 20$ K this translates to an activation energy per particle of 33 meV.

VI. Conclusion

I have discussed in some detail experimental results obtained in my laboratory and their interpretation in terms of the proton dynamics in palladium hydride. These serve as an example of our work and that of others in the application of proton magnetic resonance techniques to the study of transition metal hydrides.

VII. References

[1]H.E. Avram and R.L. Armstrong, **Can. J. Phys.** *65*, 1623-1628 (1987).

[2]H.E. Avram and R.L. Armstrong, **J. Phys. C** *18*, L833-L835 (1985).

[3]H.E. Avram and R.L. Armstrong, **Phys. Rev.** *34*, 6121-6125 (1986).

[4]H.E. Avram and R.L. Armstrong, **J. Phys. C** *17*, L89-L92 (1984).

[5]H.E. Avram and R.L. Armstrong, **J. Phys. C** *20*, 6305-6314 (1987).

[6]H.E. Avram and R.L. Armstrong, **J. Low Temp. Phys.** *69*, 391-400 (1987).